Estimating ankle joint angle from skeletal geometry: a mechanical model of the calcaneal lever in terrestrial mammals

Fumihiro Mizuno[1] and Shin-ichi Fujiwara[2]

[1] National Museum of Nature and Science, Tsukuba, Ibaraki, Japan
[2] Nagoya University Museum, Nagoya University, Nagoya, Aichi, Japan

ABSTRACT

Background: The ankle joint angle, typically measured between the tibia and metatarsus, shows only a small range of movement during the stance phase and remains relatively constant within species, but varies across taxa. This variation influences traits such as stride length, posture, and locomotor function. While joint angles are readily observable in living animals, they cannot be directly measured in extinct species, for which only skeletal remains are available. Therefore, estimating ankle joint posture from skeletal geometry is important for reconstructing locomotion in both extant and extinct mammals. In this study, we propose a mechanical model of the ankle extensor apparatus to estimate ankle joint angle from bones and test whether the muscle-lever system aligns consistently with skeletal features across taxa.

Methods: We developed a simplified mechanical model of the ankle extensor apparatus to calculate ankle extensor moment arm defined as the perpendicular distance from the ankle joint center to the muscle force line of action, which was assumed to be parallel to the tibia. To verify the Achilles tendon runs parallel to the tibia across taxa, dissections were performed on cadavers of 24 species in seven orders. We compared observed angle (θ_{obs}) from 26 species of zoo-kept terrestrial mammals, covering various body mass and locomotor modes, with estimated angle (θ_{est}) from skeletal specimens of the same species. θ_{obs} was the mean tibia–metatarsus angle during the stance phase, recorded laterally with a high-speed camera. θ_{est} was measured on reassembled skeletal specimens as the ankle joint angle that maximized the extensor moment arm in the model. Phylogenetic comparative methods, including phylogenetic ANOVA and PGLS, were applied to analyze relationships among θ_{obs}, θ_{est}, body mass, and locomotor mode based on a time-calibrated phylogeny.

Results: Dissections confirmed the Achilles tendon runs nearly parallel to the tibia across species. Stance phase ankle joint rotations were small. Therefore, θ_{obs} could be considered as representative for each species. Over 85% of the studied species maintained their ankle joint angle at which the mechanical advantage of the calcaneal lever was greater than 0.9. No significant differences in the mechanical advantage of the calcaneal lever were found among locomotor modes or taxonomic orders. A strong positive correlation was observed between θ_{obs} and θ_{est} ($\rho = 0.70$, $p < 0.001$).

Conclusion: Our mechanical model could estimate θ_{est} from skeletal morphology that closely match θ_{obs} during stance phase. Despite interspecific variation of θ_{obs}, the mechanical advantage of the calcaneal lever remains within a narrow range,

suggesting mechanical optimization of the ankle extensor apparatus across terrestrial mammals. This model informs postural reconstruction in extinct species.

INTRODUCTION

The hindlimbs perform some essential functions for terrestrial life, such as supporting body mass, generating propulsion, and lifting the body. During walking, in particular, the hindlimbs contribute to forming an inverted pendulum (*Cavagna, Heglund & Taylor, 1977*; *Alexander & Jayes, 1978a*, *1978b*; *Hildebrand, 1984*; *Hildebrand & Hurley, 1985*; *Alexander, 1991*; *Griffin, Main & Farley, 2004*) or spring-loaded inverted pendulum (SLIP) model (*Geyer, Seyfarth & Blickhan, 2006*), both of which facilitate efficient locomotion by generating propulsive energy. The SLIP model proposes that the limbs act as springs, while also emphasizing the importance of optimized stiffness (*Blickhan & Full, 1993*; *Geyer, Seyfarth & Blickhan, 2006*). In these models, the rod of the inverted pendulum is defined as the line between the grounding point of the metatarsus and the center of mass (*Cavagna, Heglund & Taylor, 1977*; *Alexander & Jayes, 1978a*, *1978b*; *Blickhan & Full, 1993*; *Griffin, Main & Farley, 2004*; *Geyer, Seyfarth & Blickhan, 2006*); therefore, the rod length is governed by the joint angles, particularly those of the knee joint and the ankle joint in the hindlimbs. The previous studies showed that the knee joint angles among mammalian species do not change drastically—remain relatively constant with small changes—during the stance phase, and differ between species (*Manter, 1938*; *Gray, 1944*; *Goslow, Reinking & Stuart, 1973*; *Goslow et al., 1981*; *Alexander & Jayes, 1983*; *Inuzuka, 1996*; *Fischer et al., 2002*; *McGowan, Baudinette & Biewener, 2005*; *Dutto et al., 2006*; *Day & Jayne, 2007*; *Ren et al., 2008*; *Patel et al., 2013*). The variations in the joint angles contribute to differences in body height, locomotion, and biology between species. However, *Mizuno & Kohno (2023)* showed that the angle between the line of the action of the *musculus semimembranosus* and the tibia resembles across mammals, even when these taxa belong to different orders. Similarly, *Fujiwara (2009)* and *Fujiwara & Hutchinson (2012)* showed that the angle between the olecranon process and the *m. triceps brachii* remains similar despite differences in the elbow joint angle typically measured between the humerus and ulna. These studies indicate that while joint angles observable from outside the body vary across species, may be conserved across mammals due to skeletal morphology. Therefore, identifying the mechanisms that determine such skeletal angles enables the reconstruction of limb postures in extinct animals, whose joint angles cannot be directly observed.

The foot is a part of the inverted pendulum of the entire hindlimb, and also functions as a lever system driven by extensor muscles to generate greater ground reaction force (*Gregory, 1912*; *Manter, 1938*; *Biewener, 1989*, *1990*; *McGowan, Baudinette & Biewener, 2005*; *Deforth et al., 2019*). The upward rotation of the calcaneal tuber, caused by contraction of these muscles, induces the downward rotation of the metatarsus, thereby generating ground reaction force. Anatomically, the extensor muscles—specifically the

m. gastrocnemius, *m. soleus*, and *m. flexor digitorum superficialis*—contribute to raising the calcaneal tuber. These extensor muscles form the *tendo calcaneus* (Achilles tendon), although the *m. soleus* is absent or weakened in some taxa. This muscle originates from the flexor side of the knee joint—specifically, the distal femur and the proximal tibia and fibula—and inserts into the distal end of the calcaneal tuber *via* the Achilles tendon, running nearly parallel to the tibia (*Kato & Yamauchi, 2003*; *König, Liebich & Bragulla, 2007*). Therefore, the net force vector produced by the extensor muscles can be assumed to run parallel to the axis of the tibia. The functional role of the ankle extensors during the stance phase to support body mass and generate propulsive force against gravity has been well established (*Engberg & Lundberg, 1969*; *Goslow, Reinking & Stuart, 1973*; *Rasmussen, Chan & Goslow, 1978*; *Walmsley, Hodgson & Burke, 1978*; *Goslow et al., 1981*; *Nicolopoulos-Stournaras & Iles, 1984*; *Whelan, Hiebert & Pearson, 1995*). In terrestrial mammals, particularly in unguligrade and digitigrade species, the ankle joint is actively extended to counteract gravitational flexion forces during both standing and stance phase. Accordingly, an extensor torque must be generated at the ankle joint, with the calcaneal tuber playing a central role in its propagation. This extensor torque arises from the force applied *via* the calcaneal tuber and the internal moment arm, defined as the perpendicular distance between the joint's center of rotation and the line of action of the muscle force (*Fujiwara, 2009*). Given this biomechanical context, it is reasonable to hypothesize that mammals adopt joint angles that maximize this moment arm during the stance phase, thereby enhancing mechanical advantage and stability.

We hypothesize that (i) the functional ankle extension angle (FAEA), defined as the angle between the line of action of the extensor muscles and calcaneal tuber, is maintained within a range that optimizes muscle force production and mechanical advantage during the stance phase of walking in terrestrial mammals; (ii) FAEA is similar among species with different observable ankle joint angle (θ) which is typically measured; and (iii) θ can be estimated from a mechanical model of the ankle extensor apparatus. This study aims to test these hypotheses using a mechanical model based on the skeletal geometry of each target species, and to provide insight into the fundamental constraints shaping limb posture, which may aid in the functional interpretation of extinct taxa.

MATERIALS AND METHODS

Mechanical model

To examine the hypotheses, we constructed a simplified mechanical model of joint rotation. For instance, the trochlea of the talus was approximated as a circular arc, and the articulations between the foot bones were assumed to be rigid. This simplification was necessary to allow general comparison across species, as skeletal morphology varies not only between species but also among individuals. Assuming the foot as a simple body of rotation about the ankle joint (Fig. 1) during extension and flexion, the ankle extensor torque (τ) is generated by the extensor muscles, which inserts at the most distal point on the calcaneus (C) (Fig. 1). τ can be expressed by the following equation:

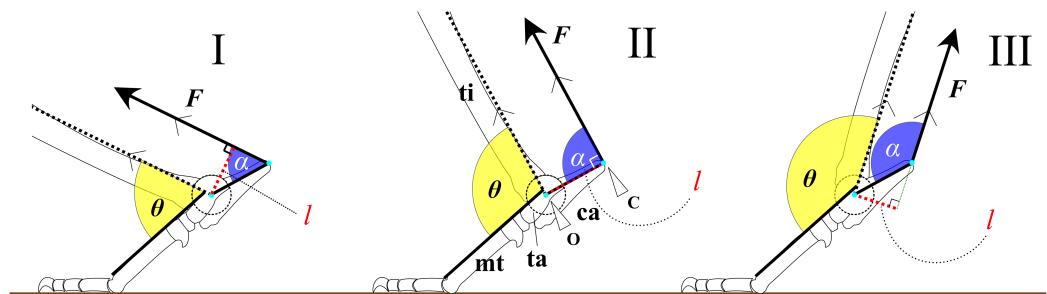$$\tau = l \times F \tag{1}$$

Figure 1 Mechanical models of the ankle extensor apparatus. Three models show (I) $a < 90°$, (II) $a = 90°$, and (III) $a > 90°$. Each yellow arc represents the ankle joint angle (θ) between the tibia and foot. Each blue arc represents the angle (a) between the line of action of the extensor muscle (F) and the line connecting the center of the ankle joint rotation (O) to the most distal point on the calcaneus (C). Each red dashed line represents the moment arm (l). θ at position (II) is defined as θ_{est}. Abbreviations: ca, calcaneus; mt, metatarsus III; and ta, talus.   Full-size ◪ DOI: 10.7717/peerj.20056/fig-1

where F is a contractile force of the extensor muscles, and l is the moment arm length. The moment arm l is defined as the perpendicular distance from the center of the ankle joint rotation (O) to the line of action of F (Fig. 1). If F is constant, τ is directly proportional to l. The moment arm l can be calculated using the following equation:

$$l = OC \cdot \sin \alpha \qquad (2)$$

where OC is the distance between O and C, and α represents the value of FAEA. Since the length OC is fixed for a given specimen, the value of l depends entirely on the angle α (Fig. 1). The function $\sin \alpha$ reaches its maximum when α is 90° (Fig. 1). Therefore, l is maximized ($\sin \alpha = 1$) when the line OC is perpendicular to the tibia and vector F. The value of $\sin \alpha$ can thus be regarded as the mechanical advantage of the calcaneal lever.

Assuming that the F runs parallel to the shaft of the tibia and that the articulations between the tarsal and metatarsal bones are rigid, we defined the estimated ankle joint angle (θ_{est}) as the angle at which $\alpha = 90°$ (Fig. 1). At this angle, the mechanical advantage of the calcaneal lever ($\sin \alpha$) is maximized. The mechanical advantage of the calcaneal lever decreases when the ankle joint angle θ deviates above or below this value θ_{est}. To investigate the directional relationship between the tibia and the Achilles tendon, anatomical observations were performed on several cadaveric specimens. Details of these observations are provided below. All angles (*e.g.*, θ and α) are expressed in degrees unless otherwise noted. θ varies depending on the specimen (Fig. 2).

Dissection

We dissected cadavers donated to the National Museum of Nature and Science (NMNS) by zoos to confirm that the Achilles tendon runs parallel to the tibia, and that the orientation is consistent across different species. The species dissected belong to seven orders, 23 genera, and 24 species (Table 1). All individuals were adults. We followed the ethical guidelines of the NMNS during the dissection.
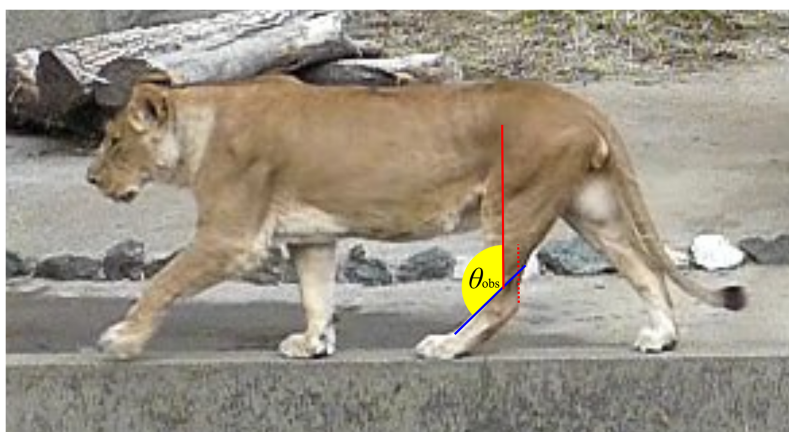
Figure 2 An example image used to collect ankle joint angle data from living individuals. The red dashed line represents the Achilles tendon, while the red solid line indicates the tibial shaft, which runs parallel to the Achilles tendon. The blue solid line shows the dorsal margin of the third metatarsal (metatarsus III). The yellow fan illustrates the ankle joint angle (θ_{obs}) being measured.

Table 1 A list of dissected species by first author.

Species	Location
Artiodactyla	
Bos taurus	NMNS
Capricornis crispus	NMNS
Cervus nippon yakusimae	NMNS
Elaphurus davidianus	NMNS
Giraffa camelopardalis	NMNS
Rangifer tarandus	NMNS
Perissodactyla	
Equus caballus (pony)	NMNS
Equus zebra	NMNS
Tapirus terrestris	KPM
Carnivora	
Aonyx cinerea	NMNS
Acinonyx jubatus	NMNS
Canis lupus familialis	NMNS
Chrysocyon brachyurus	NMNS
Panthera leo	NMNS
Suricata suricatta	NMNS
Vulpes vulpes	NU
Primates	
Cercopithecus neglectus	NMNS
Erythrocebus patas	NMNS
Macaca fuscata	NMNS

(Continued)

Table 1 (continued)	
Species	**Location**
Rodentia	
Castor canadensis	NMNS
Dolichotis patagonum	NMNS
Galea musteloides	NMNS
Diprotodontia	
Petrogale xanthopus	NMNS

Note:
Abbreviations: NMNS, National Museum of Nature and Science, Tsukuba, Japan; KPM, Kanagawa Prefectural Museum of Natural History, Odawara, Japan; NU is Japan University, Nagoya, Japan.

Collection from living individuals

We defined the ankle joint (θ_{obs}) as the angle between the tibia and the metatarsus III of living individuals. Data were collected from 26 extant species, including two domestic breeds (Kiso Horse and thoroughbred) within *Equus caballus*. Thus, the total number of species was 26, representing 25 genera and 16 families across nine orders (Table 2). These species were selected to cover a wide range of taxa, body masses (*i.e.*, from 0.06 kg for the Mongolian gerbil to 3,400 kg for white rhinoceros), and locomotor mode (unguligrade, digitigrade, plantigrade, and pentapedal) (Table 2). Pentapedal locomotion refers to the mode used by kangaroos (O'Connor et al., 2014). Most target animals are kept in zoos at Higashi Park Zoological Gardens (Aichi, Japan), Higashiyama Zoo and Botanical Garden (Aichi, Japan), Hitachi Kamine Zoo (Ibaraki, Japan), Toyohashi Zoo and Botanical Park (Aichi, Japan), and Ueno Zoological Gardens (Tokyo, Japan), and all observations were conducted with official permissions from these facilities. Mongolian gerbils and a cat were kept by a colleague of the authors, and the thoroughbred was hosed at the equestrian arts club of Tsukuba University Equestrian Team (University of Tsukuba). No individuals showed significant pathologies or malformations. Furthermore, we avoided using juvenile individuals.

High-speed video recordings (420 fps) were obtained using a Casio EX-FH20 digital camera (Japan) mounted on a tripod positioned along public viewing paths. The distance between the camera and the targets varied depending on the exhibition/cage layout. All videos were taken from the lateral side and at nearly the same level as each target animal when they walked voluntarily in a straight line without stopping, turning, or changing speed, and perpendicular to the camera on flat ground. No external stimuli (handlers, markers, and confinement) were applied, and recordings were made passively. Kangaroos were recorded while pentapedal locomotion, which use four legs and a tail, rather than hopping. Some data were cited from previous studies (Table 2).

We defined one stance phase, from touch-down to take-off, as one step during stance phase. Each step was screen-captured from the videos using GOM player (Gretech Corporation, Seoul, South Korea). The captured images of each step were divided into five equal time intervals to yield six images per stance phase. On each of the six images, two lines were drawn using Inkscape (ver. 1.2, Inkscape Project), and the angle between them

Table 2 List of the studied species, with the number of the steps used for the analysis, the locations where the data of the steps were collected, number of the skeletal specimens used for the measurements, and the list of the specimens.

Order, Family	Species (common name)	Steps [n]	Locality or reference	Skeletons [n]	Specimen
Artiodactyla					
Bovidae					
	Ammotragus lervia (Barbary sheep)	2	UZ	1	NMNS M42950
	Capra hircus (goat)	4	Co1	1	KPM NF-1004771
	Capricornis crispus (Japanese serow)	2	HZBG	3	NMNS M34472; NMNS M35895; TMNH MA304
Cervidae					
	Cervus nippon yesoensis (Yezo shika deer)	2	UZ	1	NMNS M39257
	Rangifer tarandus (reindeer)	2	HZBG	2	NMNS M31343; NMNS M34433
Giraffidae					
	Giraffa reticulata (reticulated giraffe)	9	UZ	3	NMNS M33232; NMNS M34445; NMNS M47162
Hippopotamidae					
	Choeropsis liberiensis (pygmy hippopotamus)	3	UZ	1	NMNS M36955
Perissodactyla					
Equidae					
	Equus caballus (Kiso horse)	3	TZBP	1	NMNS M31212
	Equus caballus (thoroughbred)	3	TET	2	NMNS M75179; NMNS M77948
Rhinocerotidae					
	Ceratotherium simum (white rhinoceros)	2	TZBP; *Day & Jayne (2007)*	3	NMNS M31319; NMNS M31455; NMNS M37727
	Rhinoceros unicornis (Indian rhinoceros)	5	HZBG	1	KPM NF1002747
Tapiridae					
	Tapirus terrestris (South American tapir)	2	HZBG	2	NMNS M31505; OMNH unnumbered
Carnivora					
Canidae					
	Canis lupus (wolf)	4	HZBG	2	NMNS M43287; OMNH M440
	Chrysocyon brachyurus (maned wolf)	3	UZ	2	NMNS M36655; NMNS M53024
Felidae					
	Acinonyx jubatus (cheetah)	(125)	*Day & Jayne (2007)*	2	NMNS M31465: NMNS M37279

(Continued)

Table 2 (continued)

Order, Family	Species (common name)	Steps [n]	Locality or reference	Skeletons [n]	Specimen
	Felis silvestris catus (cat)	3	Co1	3	NMNS M36028; NMNS M36030; NMNS M76763
	Panthera leo (lion)	6 (119)	TZBP; *Day & Jayne (2007)*	3	NMNS M37728; NMNS M42648; NMNS M43347
	Panthera tigris (Sumatran tiger)	3 (125)	HZBG; *Day & Jayne (2007)*	4	NMNS M38483; NMNS M38486; OMNH M2401; TMNH MA318
Herpestidae					
	Suricata suricatta (meerkat)	3	HZBG	2	NMNS 33399; NMNS M54629
Primates					
Cercopithecidae					
	Cercopithecus neglectus (De Brazza's monkey)	2	UZ	2	NMNS M71712; NMNS M75202
	Macaca fuscata (Japanese macaque)	3	KZ	3	NMNS M36028; NMNS M36074; NMNS M63048
Rodentia					
Caviidae					
	Dolichotis patagonum (Patagonian mara)	2	HPZG	3	NMNS M35595; NMNS M35760; NMNS M35880
	Galea musteloides (yellow-toothed cavy)	(73)	*Fischer et al. (2002)*	1	NMNS M36015
Muridae					
	Meriones unguiculatus (Mongolian gerbil)	2	Co2	1	NMNS M11702
Scandentia					
Tupaiidae					
	Tupaia glis (common tree shrew)	(84)	*Fischer et al. (2002)*	1	NMNS M28531
Diprotodontia					
Macropodidae					
	Macropus fuliginosus (western grey kangaroo)	1	HZBG	1	NMNS M43349
	Macropus giganteus (eastern grey kangaroo)	3	UZ	1	NMNS M43210

Note:
Abbreviations for the locality: Co1 and 2, colleagues who keep the animal; HZBG, Higashiyama Zoo and Botanical Garden, Nagoya, Japan; KZ, Hitachi Kamine Zoo, Hitachi, Japan; TET, Tsukuba University Equestrian Team, Tsukuba, Japan; TZBP, Toyohashi Zoo and Botanical Park, Toyohashi, Japan; UZ, Ueno Zoological Garden, Tokyo, Japan.
Abbreviations for the museums: NMNS, National Museum of Nature and Science, Tsukuba, Japan; KPM, Kanagawa Prefectural Museum of Natural History, Odawara, Japan; OMNH, Osaka Museum of Natural History, Osaka, Japan.

was measured: one line extended from the ankle joint and the proximal end of the tibia, parallel to the Achilles tendon, and the other line along the dorsal margin of the metatarsus III (Fig. 2). We used three or more steps for 13 species, two steps for nine species, and one step for one species, from videos. In addition, five species were cited from previous studies including three species for which both our video data and previous studies were used (Table 2). The mean of the measured angles was defined as θ_{obs}.

Collection from skeletal specimens

The ankle joint angles at which the extensor moment arm is maximized were measured using skeletal specimens. The data were collected for the same 26 species used in the observations of θ_{obs} (Table 2). Disarticulated hindlimb bones stored at the National Museum of Nature and Science (NMNS: Tsukuba, Japan), Toyohashi Museum of Natural History (Toyohashi, Japan), Kanagawa Prefectural Museum of Natural History (Odawara, Japan), and Osaka Museum of Natural History (Osaka, Japan) (Table 2) were used. A total of 42 skeletal specimens were measured. No specimens showed significant pathologies or malformations. Furthermore, we avoided using juvenile specimens.

We reassembled the metatarsals and tarsal bones (calcaneus, talus, cuneiforms, navicular, and cuboid) using a soft, reusable adhesive (Hittsukimushi, Kokuyo, Osaka, Japan), and then the flexibility of the joint connections was confirmed to be negligibly small. The Mongolian gerbil foot skeleton was stored with the bones connected by tendons and ligaments. The reassembled bones were photographed in lateral view using a digital camera (D3400; Nikon, Tokyo, Japan).

Two lines were then drawn on each image, and the angle between them was measured following procedure described below. First, a circle centered at O, which best fits the ridge of the trochlea of the talus, was drawn. Next, a perpendicular line (line A) to the line segment OC, originating from point O, was drawn. Following this, a line connecting the dorsal tips of the proximal and distal epiphyses on the metatarsal III (line B) was drawn (see description in Mechanical Model section). Finally, the angle between lines A and B was defined as the ankle joint angle where the extensor moment arm maximized for the specimen (Fig. 3). These figures were also created using Inkscape. The average of the angles for each species was defined as θ_{est}.

Statistical analysis

For statistical analysis, body mass (in grams) was transformed using natural logarithmic scale (ln). The locomotor mode was classified into four groups: plantigrade, digitigrade, unguligrade, and pentapedal (Table 2). Phylogenetic Comparative Methods (PCMs) were applied to all measurements and derived variables. Pairwise comparisons were conducted following the phylogenetic ANOVA (phyANOVA) using phylogenetic t-tests with Holm's correction for multiple testing to determine which pairs had significant differences (*Garland et al., 1993*; *Revell, 2012*). Additionally, the correlation coefficient between θ_{obs} and θ_{est} was calculated.

Phylogenetic generalized least squares (PGLS) analyses were performed to examine the following relationships: (1) mechanical advantage of the calcaneal lever and locomotor
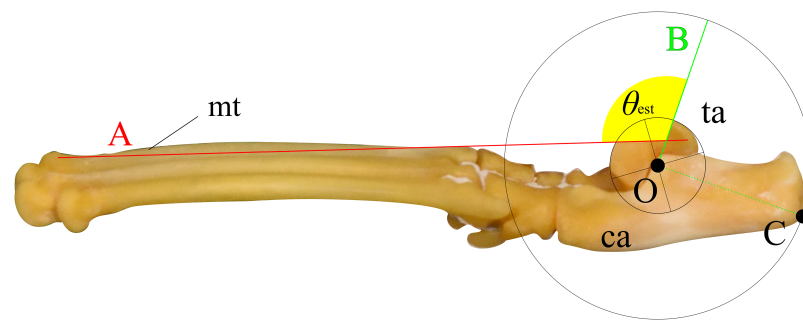
Figure 3 An example of the picture for measuring the ankle joint angle data from the skeletal specimens using a cat (M36028). The foot element in connection (tarsal and metatarsal bones) is photographed from the medial view. Point O represents the center of a circle that best fits the edge of the trochlea of the talus. Point C indicates the contact point on the calcaneus when the concentric circle reaches its maximum size. Line A connects the dorsal edges of the proximal and distal epiphyses of metatarsal III. Line B is drawn perpendicular to the line segment OC, originating from point O. The yellow fan represents the measured ankle joint angle (θ_{est}). Abbreviations: ca, calcaneus; mt, metatarsus III; and ta, talus. The scale bar is 10 mm. This foot was rearticurated and taken by the author at NMNS.
Full-size 🖼 DOI: 10.7717/peerj.20056/fig-3

mode; (2) mechanical advantage of the calcaneal lever and body mass; and (3) body mass, θ_{obs} and θ_{est}. The phylogenetic tree used for these analyses was constructed using Timetree: The Timescale of Life (https://timetree.org/).

All statistical analyses were performed using the R software package (ver. 4.4.1, *R Core Team, 2024*).

RESULTS

The directions of the Achilles tendon and the tibia were nearly parallel in the species dissected in this study (Fig. 4). This parallel orientation of the Achilles tendon relative to the tibia was consistently observed over a wide range of joint angles. Therefore, the direction of the line of action of the ankle joint extensor muscle can be approximated by the tibia. Additionally, the transitions of the ankle joint angle during the stance phase were checked to ensure the θ_{obs} represented the angle of the target species. According to the line graph of the ankle joint angle transitions, these were gradual and the maximum differences between the average angle (θ_{obs}) and the maximum or minimum angle were small in the many studied species (Fig. 5): in 22 species of the 27 studied species, the maximum differences were less than 20 degrees. Thus, θ_{obs} was considered representative for each species and was suitable for comparison with θ_{est}. The Mongolian gerbil which had the smallest body mass, 0.06 kg, had both the minimum θ_{obs} and θ_{est} (64° and 95°, respectively). The white rhinoceros, which has the largest body mass, 3,400 kg, had the second maximum θ_{est} (141°). Thoroughbred, with the fourth largest body mass (518 kg), had the maximum θ_{obs} (157°), whereas the maximum θ_{est} was 146° for the Indian rhinoceros, which had the second largest body mass (2,100 kg) (Table 3). The Japanese serow, reindeer, and Japanese macaque had the smallest absolute difference between θ_{est} and θ_{obs} (0°), and the thoroughbred had the largest difference, 38° (Table 3).
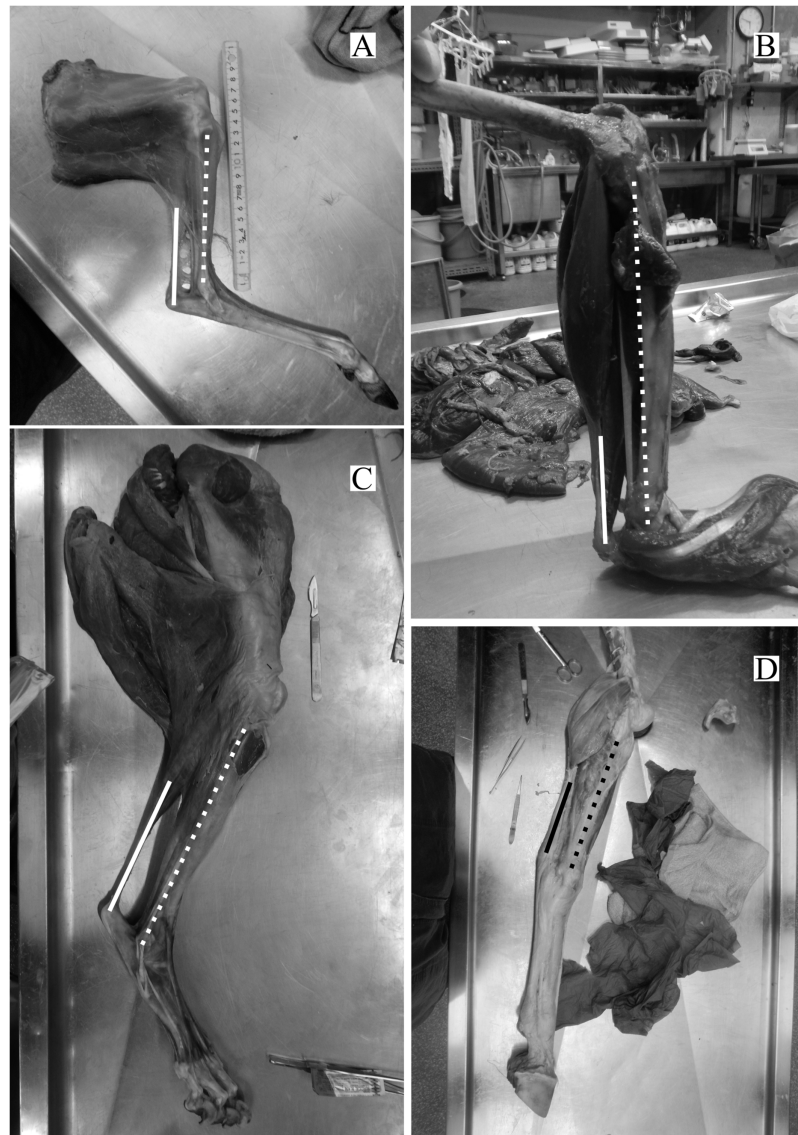
Figure 4 Some examples of the hind limbs dissected by first author. (A) *Cervus nippon yakusimae*; (B) *Macaca fuscata*; (C) *Panthera leo*; (D) *Equus caballus* (pony). Solid lines show the Achilles tendon, and broken lines showed the shaft of the tibia. Note that these lines run nearly parallel with each other. The author performed the dissections and took these photos at NMNS.

Full-size 🖼 DOI: 10.7717/peerj.20056/fig-4

In 24 species (including the Kiso horse), the value of the mechanical advantage of the calcaneal lever exceeded 0.9; among these, 18 species had values greater than 0.95. Three species had the mechanical advantage of the calcaneal lever between 0.8 and 0.9. The thoroughbred had the lowest mechanical advantage of the calcaneal lever at 0.79 (Table 3 and Fig. 6). PhyANOVA and pairwise comparisons were conducted to assess significant differences in the mechanical advantage of the calcaneal lever among locomotor modes. The phyANOVA showed no significant differences ($p = 0.602$), and all pairwise Holm-adjusted p-values were equal to 1.00; therefore no significant differences in the
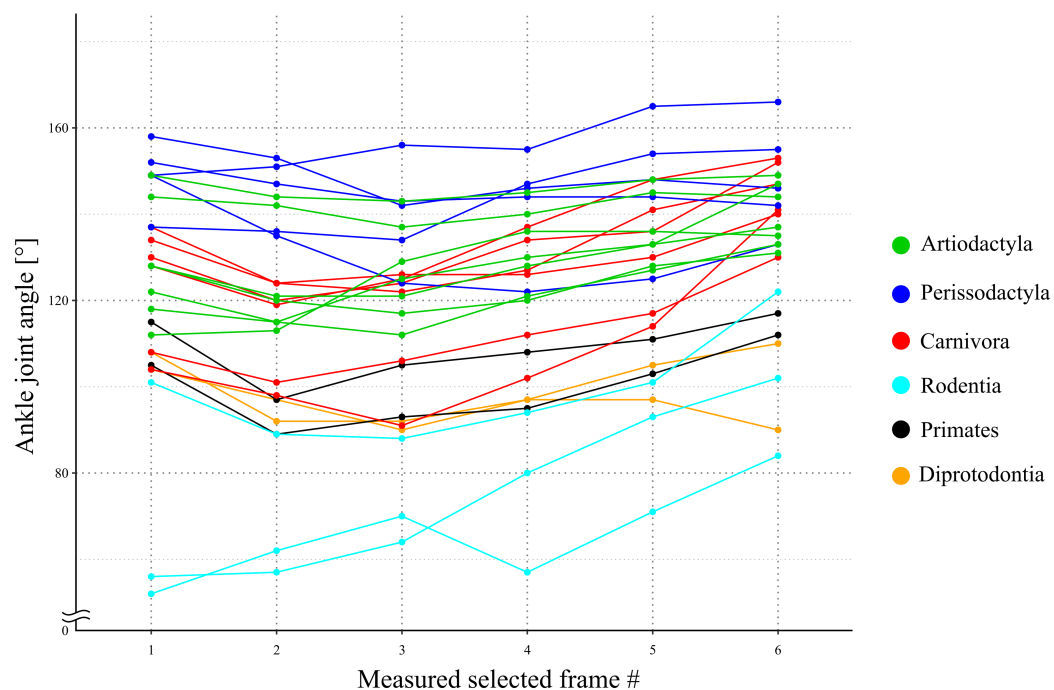
Figure 5 A line graph of the angle transition of target animals. X-axis shows the number of the measured selected frames between the beginning and the end of the stance phase. Y-axis shows the ankle joint angle. The averages of these angles were defined as θ_{obs} [°] for each species. Each color shows the taxonomic group (order) of the target animals and the representation of each color in the legend.

Full-size 🖼 DOI: 10.7717/peerj.20056/fig-5

Table 3 The values of the observed ankle joint angle (θ_{obs}), estimated ankle joint angle (θ_{est}), efficiency of the calcaneal lever of the ankle joint extensor (sin α), body mass, and locomotor mode of the studied species.

Order	Family	Species	θ_{obs} (°)	θ_{est} (°)	sin α	Body mass (kg)	Locomotor mode
Artiodactyla	Bovidae	*Ammotragus lervia*	142	130	0.98	64	U
		Capra hircus	130	137	0.99	20	U
		Japanese serow	127	127	1.00	38	U
	Cervidae	*Capricornis priscus*	126	123	0.99	75	U
		Rangifer tarandus	122	121	1	120	U
	Giraffidae	*Giraffa reticulata*	146	140	0.99	1,000	U
	Hippopotamidae	*Choeropsis liberiensis*	124	117	0.99	223	U
Perissodactyla	Equidae	*Equus caballus*: Kiso horse	144	125	0.95	400	U
		Equus caballus: thoroughbred	157	119	0.79	518	U
	Rhinocerotidae	*Ceratotherium simum*	149	141	0.99	3,400	U
		Rhinoceros unicornis	145	146	1.00	2,100	U
	Tapiridae	*Tapirus terrestris*	131	102	0.87	200	U
Carnivora	Canidae	*Canis lupus*	130	119	0.98	40	D
		Chrysocyon brachyurus	133	124	0.98	24	D

Table 3 (continued)

Order	Family	Species	θ_{obs} (°)	θ_{est} (°)	sin α	Body mass (kg)	Locomotor mode
	Felidae	*Acinonyx jubatus*	125	112	0.97	48	D
		Felis silvestris catus	112	109	0.99	4.8	D
		Panthera tigris	125	114	0.98	125	D
		Panthera leo	120	108	0.98	188	D
	Herpestidae	*Suricata suricatta*	108	121	0.98	0.7	D
Primates	Cercopithecidae	*Cercopithecus neglectus*	99	108	0.99	4.5	P
		Macaca fuscata	109	109	1.00	16	P
Rodentia	Caviidae	*Dolichotis patagonum*	99	111	0.98	8	D
		Galea musteloides	75	106	0.86	0.34	P
	Muridae	*Meriones unguiculatus*	66	95	0.88	0.06	P
Scandentia	Tupaiidae	*Tupaia glis*	84	107	0.92	0.18	P
Diprotodontia	Macropodidae	*Macropus fuliginosus*	96	119	0.92	43.5	Pe
		Macropus giganteus	101	122	0.93	41	Pe

Note:
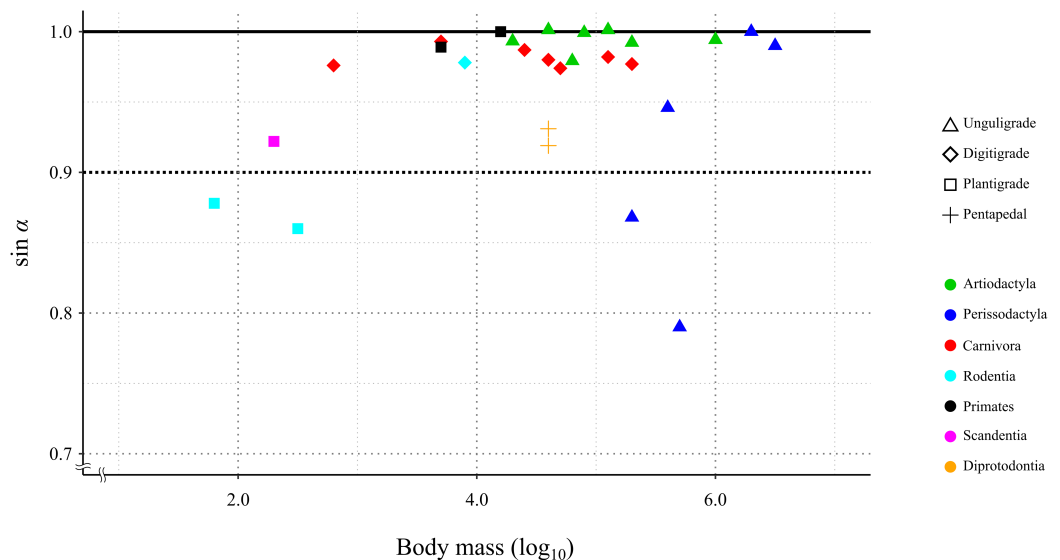Abbreviations for the locomotor modes: D, digitigrade; P, plantigrade; Pe, pentadactyl; U, unguligrade.

Figure 6 Relationship between the efficiency of the calcaneus lever (sin *a*) during the stance phase in the studied species. X-axis shows the body mass in $\log_{10}$. Y-axis shows the value of sin α. See legends for the taxonomic group (order) of the target animals (color-code) and the locomotor mode (symbol shape). Full-size ⤢ DOI: 10.7717/peerj.20056/fig-6

mechanical advantage of the calcaneal lever among locomotor modes (Table 4). Additional phyANOVA and pairwise comparisons were also conducted among orders. However, since Scandentia was represented by only one species, it was excluded from the analysis. The phyANOVA among orders also showed no significant differences ($p = 0.665$), and all pairwise Holm-adjusted p-values were equal to 1.00 (Table 4). Thus, neither locomotor

Table 4 Results of phyANOVA for the relationships between locomotor modes and the efficiency of the calcaneal lever of the ankle joint extensor (sin α), and between taxonomic order and sin α.

PhyANOVA (Locomotor mode *vs.* sin α)

	Sum Sq	Mean Sq	*F* value	*p*-value
Locomotor mode	0.0143	0.0048	3.4994	0.618
Residual	0.0299	0.0014	—	—
Pairwise posthoc test				
Comparison			Adjust *p*-value	
Digitigrade *vs.* Unguligrade			1	
Digitigrade *vs.* Plantigrade			1	
Digitigrade *vs.* Pentapedal			1	
Unguligrade *vs.* Plantigrade			1	
Unguligrade *vs.* Pentapedal			1	
Plantigrade *vs.* Pentapedal			1	

PhyANOVA (Order *vs.* sin α)

	Sum Sq	Mean Sq	*F* value	*p*-value
Order	0.0240	0.0048	5.068	0.661
Residual	0.0180	0.0009	—	—
Pairwise posthoc test				
Comparison			Adjust *p*-value	
Artiodactyla *vs.* Perissodactyla			1	
Artiodactyla *vs.* Carnivora			1	
Artiodactyla *vs.* Primates			1	
Artiodactyla *vs.* Rodentia			1	
Artiodactyla *vs.* Diprotodontia			1	
Perissodactyla *vs.* Carnivora			1	
Perissodactyla *vs.* Primates			1	
Perissodactyla *vs.* Rodentia			1	
Perissodactyla *vs.* Diprotodontia			1	
Carnivora *vs.* Primates			1	
Carnivora *vs.* Rodentia			1	
Carnivora *vs.* Diprotodontia			1	
Primates *vs.* Rodentia			1	
Primates *vs.* Diprotodontia			1	
Rodentia *vs.* Diprotodontia			1	

mode nor order showed significant differences in the mechanical advantage of the calcaneal lever.

Since the mechanical advantage of the calcaneal lever was not normally distributed, the Spearman's rank order correlation was used to assess the correlation coefficient. The correlation coefficient between the θ_{obs} and the θ_{est} was 0.75, with the *p*-value less than 0.05 ($p = 1.21 \times 10^{-5}$: Table 4 and Fig. 7). This indicated a strong positive correlation between θ_{obs} and θ_{est}, and supporting a significant correlation in the population.
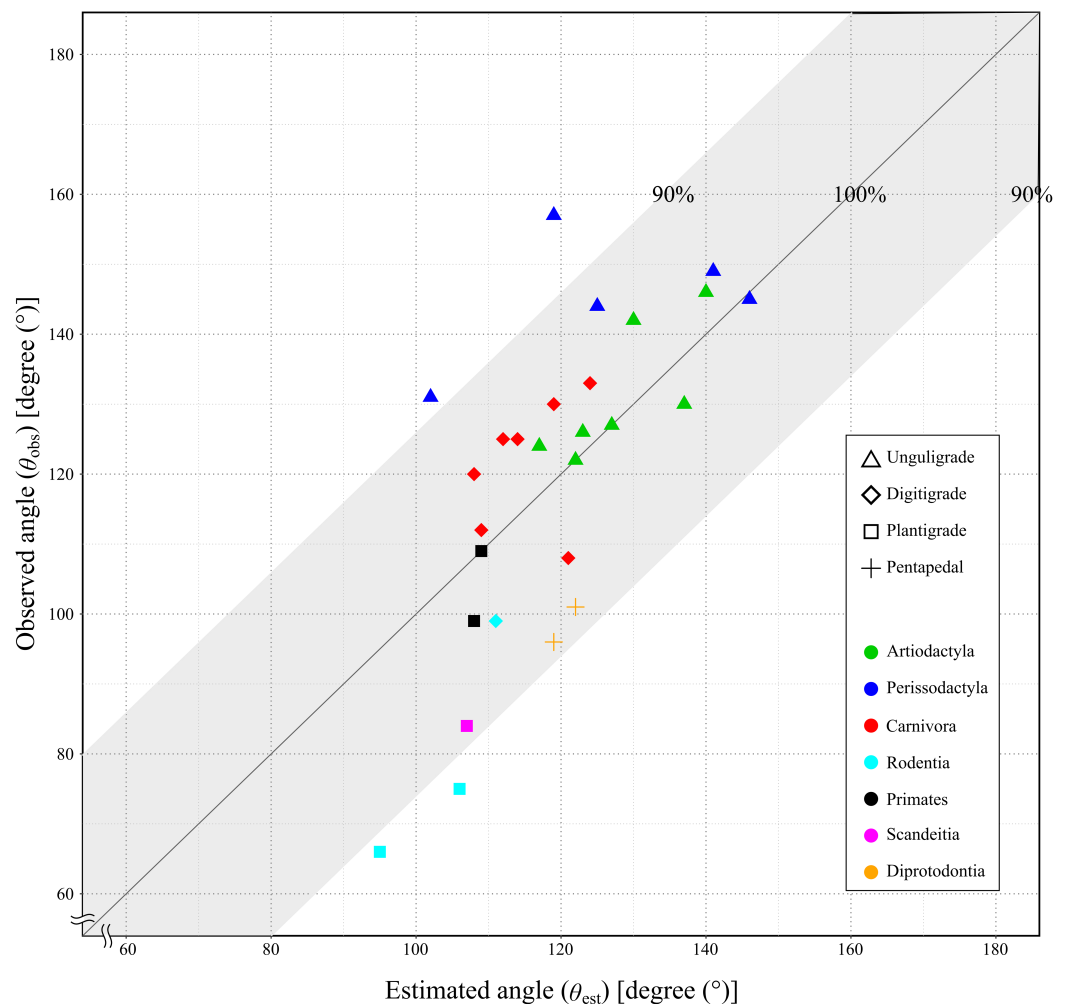
Figure 7 Relationship between the observed angle (θ_{obs}) and the estimated angle (θ_{est}) in studied species. X-axis shows the estimated angle (θ_{est}). Y-axis shows the observed angle (θ_{obs}). The gray area shows the lever of the ankle joint exerts more than 90%. See legends for the taxonomic group (order) of the target animals (color-code) and the locomotor mode (symbol shape).

Full-size 🖼 DOI: 10.7717/peerj.20056/fig-7

We also performed multiple linear regression analysis *via* PGLS using three data sets: (1) Kiso horse data representing horse; (2) thoroughbred data representing horse; and (3) excluding horse to examine the relationships between θ_{obs}, θ_{est}, and body mass. This approach was taken because the mechanical advantage of the calcaneal lever values differed notably between the Kiso horse and the thoroughbred, even though they belong to same species (Table 3). The regression equation for the θ_{obs} can be expressed as:

$$\theta_{obs} = \beta_0 + \beta_1 \cdot \theta_{est} + \beta_2 \cdot \text{body mass} \tag{3}$$

In the Kiso horse data set, the regression coefficients were $\beta_0 = 4.90$ (95% confidence interval (CI) [−34.25 to 43.05], intercept), $\beta_1 = 0.48$ (95% CI [0.12–0.83], coefficient for θ_{est}, $p = 0.009$), and $\beta_2 = 4.87$ (95% CI [3.10–6.25], coefficient for body mass, $p = 2.9 \times 10^{-6}$), with a significant overall model ($p = 6.1 \times 10^{-8}$, adjusted $R^2 = 0.74$) (Table 5). In the

Table 5 Results of PGLS of observed ankle joint angle (θ_{obs}) as a function of estimated ankle joint angle (θ_{est}) and body mass (ln).

PGLS of θ_{obs} as a function of θ_{est} and body mass (ln)

Dataset	Predictor	Estimate	Std. Error	t value	p value	Pagel's λ
Kiso horse	Intercept	4.90	18.94	0.26	0.798	0.943
	θ_{est}	0.48	0.17	2.84	0.009	
	Body mass	4.87	0.76	6.14	2.89×10^{-6}	
Thoroughbred	Intercept	8.42	21.99	0.38	0.705	0.977
	θ_{est}	0.43	0.19	2.28	0.032	
	Body mass	4.87	0.86	5.68	8.7×10^{-6}	
Excluding horse	Intercept	5.46	18.75	0.29	0.773	0.938
	θ_{est}	0.47	0.17	2.85	0.009	
	Body mass	4.61	0.76	6.08	4.0×10^{-6}	

Thoroughbred data set, the coefficients were $\beta_0 = 8.42$ (95% CI [−37.85 to 54.69]), $\beta_1 = 0.43$ (95% CI [0.03–0.83], $p = 0.032$), and $\beta_2 = 4.87$ (95% CI [3.07–6.67], $p = 8.7 \times 10^{-6}$) (overall model $p = 6.7 \times 10^{-7}$, adjusted $R^2 = 0.68$) (Table 5). In the data set excluding *Equus caballus*, the coefficients were $\beta_0 = 5.46$ (95% CI [−33.30 to 44.22]), $\beta_1 = 0.47$ (95% CI [0.12–0.82], $p = 0.009$), and $\beta_2 = 4.61$ (95% CI [2.97–6.25], $p = 4.0 \times 10^{-6}$) (overall model $p = 9.5 \times 10^{-8}$, adjusted $R^2 = 0.75$) (Table 5). Pagel's λ values indicated a strong phylogenetic signal across all data sets (0.943, 0.977, and 0.938, respectively) (Table 5).

DISCUSSION

A total of 85.2% (23 out of 27) of the studied species showed a mechanical advantage of the calcaneal lever greater than 0.9 (sin α > 0.9). This species included individuals with a wide range of body masses, from 0.18 kg (common tree shrew) to 3,400 kg (white rhinoceros), as well as species representing three locomotor modes and six orders (Table 3). The phyANOVA and pairwise comparison tests for mechanical advantage of the calcaneal lever across locomotor modes and taxonomic orders detected no significant differences. Additionally, the correlation coefficient between mechanical advantage of the calcaneal lever and body mass was not statistically significant ($p = 0.12$), suggesting that the mechanical advantage of the calcaneal lever is not strongly influenced by these factors. These results suggest that FAEA of terrestrial mammals is maintained within a range that optimizes mechanical advantage of the calcaneal lever during the stance phase under steady-speed walking conditions, across a wide range of body masses and taxa. A higher mechanical advantage of the calcaneal lever enhances torque generation at the ankle joint for a given muscle force, contributing to more efficient support and propulsion during walking (*Biewener, 1989*; *Biewener & Roberts, 2000*; *Ray & Takahashi, 2020*). This mechanical advantage is particularly important during the stance phase, when joints must resist gravitational flexion forces.

Based on the multiple linear regression analyses using PGLS, the Kiso horse data set more closely resembled the excluding *E. caballus* data set (Table 5); therefore, the Kiso

Table 6 The ln of body mass (BM), mechanical advantage of the calcaneal lever (sin α), observed (θ_{obs}) and estimated (θ_{est}) ankle joint angles, the difference between θ_{obs} and θ_{est} (θ[sub]).

Species	ln BM	sin α (mechanical advantage)	θ_{obs}	θ_{est}	$\theta_{obs}-\theta_{est}$	$\theta_{r\text{-}obs}$	$\theta_{obs}-\theta_{r\text{-}obs}$
Meriones unguiculatus	4.1	0.87	66	95	−29	69	−3
Tupaia glis	5.2	0.92	84	107	−23	80	4
Galea musteloides	5.8	0.86	75	106	−31	83	−8
Suricata suricatta	6.6	0.99	108	121	−13	93	15
Cercopithecus neglectus	8.4	0.99	99	108	−9	96	3
Felis silvestris catus	8.5	1.00	112	109	3	96	16
Dolichotis patagonum	9.0	0.98	99	111	−12	100	−1
Macaca fuscata	9.7	1.00	109	111	−2	103	6
Capra hircus	9.9	0.99	130	137	−7	116	14
Chrysocyon brachyurus	10.1	0.99	133	124	9	111	22
Canis lupus	10.5	0.98	130	119	11	111	19
Capricornis crispus	10.6	1.00	127	127	0	115	12
Macropus fuliginosus	10.6	0.92	96	119	−23	111	−15
Macropus giganteus	10.7	0.93	101.	122	−21	113	−12
Acinonyx jubatus	10.8	0.97	125	112	13	109	16
Ammotragus lervia	11.1	0.98	142	130	12	118	24
Cervus nippon yesoensis	11.2	1.00	126	123	3	116	10
Panthera tigris	11.7	0.98	125	114	11	114	11
Rangifer tarandus	11.7	1.00	121	122	−1	118	3
Choeropsis liberiensis	12.1	0.99	124	117	7	117	7
Panthera leo	12.2	0.98	120	108	12	113	7
Tapirus terrestris	12.3	0.88	131	103	28	111	20
Equus caballus: Kiso horse	12.9	0.95	144	125	19	125	19
Equus caballus: thoroughbred	13.2	0.79	157	119	38	123	34
Giraffa reticulata	13.8	0.99	146	140	6	136	10
Rhinoceros unicornis	14.6	1.00	145	146	−1	142	3
Ceratotherium simum	15.0	0.99	149	141	8	142	7

horse data set was treated as representative of *E. caballus*. The regression equation showed that the effect of body mass on θ_{obs} is notably stronger than that of θ_{est}, where each unit increase in θ_{est} leads to an increase in θ_{obs} by about 0.48 degrees. Both factors significantly influence θ_{obs}, with body mass having a more substantial impact. However, in species exceeding 10 kg in body mass, the recalculated θ_{obs} values using the regression equation (hereafter referred to as $\theta_{r\text{-}obs}$) showed larger differences from θ_{obs} than differences of θ_{est} values. These mean values were 11.1 and 6.0 degrees, respectively. The $\theta_{r\text{-}obs}$ values showed smaller differences than θ_{est} in 11 out of 26 species, but five of these 11 species had a body mass below 10 kg (Mongolian gerbil, common tree shrew, yellow-toothed cavy, meerkat, and cat) (Table 6). Notably, only seven out of the 26 species had a body mass below 10 kg (Table 6). Among the 19 species exceeding 10 kg, three species (pygmy hippopotamus, tiger, and Kiso horse) showed identical differences from the θ_{obs} for both $\theta_{r\text{-}obs}$ and θ_{est}. In

the remaining 16 species, θ_{est} showed smaller differences than $\theta_{r\text{-}obs}$ in 11 cases. On average differences of $\theta_{r\text{-}obs}$ were 3.8 degrees in species below 10 kg, and 11.1 degrees in species exceeding 10 kg. In contrast, the differences in θ_{est} were −16.3 degrees in species below 10 kg, and 6.0 degrees in species exceeding 10 kg (Table 6). In addition, the correlation coefficient between the θ_{obs} and the θ_{est} was significantly positive and strong ($r = 0.74$). Therefore, θ_{est} can be reliably used to reconstruct θ_{obs} in species exceeding 10 kg, even if the skeletal specimens have been stored disarticulated.

Notably, kangaroos (*Macropus* spp.) showed negative values for θ_{obs} minus θ_{est} (−23 and −21, respectively) (Table 6), indicating that the θ_{obs} were more flexed than the θ_{est}. Kangaroos employ a unique form of locomotion known as pentapedal, which uses the tail to support body mass during quadrupedal walking (*Windsor & Dagg, 1971*; *O'Connor et al., 2014*). However, because the tail is used during the swing phase of the hindlimbs, other factors may contribute to this result. One possible explanation is that quadrupedal walking is not the typical mode of locomotion for them; they primarily use hopping as their main mode of locomotion. The hopping gait is most commonly employed during regular movement, escape responses, and long-distance travel (*Windsor & Dagg, 1971*; *O'Connor et al., 2014*). Their hindlimbs are highly specialized for hopping, *e.g.*, elongated metatarsals and shortened forelimbs (*Alexander & Vernon, 1975*; *Polly, 2007*; *McGowan & Collins, 2018*; *Jones, Travouillon & Janis, 2024*). The elongated metatarsals of hopping species increase the distance between the ground and the ankle joint, whereas short forelimbs reduce the distance between the ground and the trunk. It is possible that flexion of the hindlimb joints during quadrupedal walking, as observed in this study, serves to lower the posterior trunk, which might partly account for the more flexed θ_{obs} relative to θ_{est} in kangaroos. However, because this study includes two kangaroos species, additional data from other hopping species such as wallaby and kangaroo rat are needed to confirm the idea.

The data from two breeds of horses, the Kiso horse and the thoroughbred, implied that artificial selection had influenced on their morphology. These two breeds are classified in the same species, *Equus caballus* (horse), but their sin α differed by 0.16, with the Kiso horse showing higher value (0.95) than the Thoroughbred (0.75) (Table 3). This difference was greater than between the highest and the second lowest sin α of this study, 0.13 (Table 3). This difference appeared to result from more extended hindlimb posture in thoroughbred, where θ_{obs} exceeded θ_{est}, reducing the mechanical advantage of the calcaneal lever. While both breeds are domesticated, their morphology reflects fundamentally different breeding purposes. The Kiso horse is a medium-sized Japanese native horse that had been raised since around fifth century and used for agriculture and transportation in mountain regions until the middle of the 20th century (*Nakagawa, 2014*; *Yamashita, 2014*). Today, it is maintained primarily for conservation. In addition, the Japanese native horses have remained independent from modern breeding (*Nozawa, 1992*). Thoroughbred, on the other hand, was developed in the late 18th century and has been strongly selected for racing abilities and characteristics until today (*Cunningham, 1991*; *Bower et al., 2012*). It is possible that artificial selection for enhanced galloping ability in Thoroughbreds has favored morphologies that maximize propulsion during high-speed

locomotion. This may include joint configurations that enhance the rotational torque around the ankle joint (*Gnagey, Clayton & Lanovaz, 2006*). Additionally, efficient elastic energy storage requires significant tendon stretch, which is facilitated by joint flexion (*Dimery, Alexander & Ker, 1986*; *Biewener, 1998*). Therefore, more extended posture during walking of thoroughbred may reflect an adaptation for maximize both elastic energy recovery and mechanical advantage of the calcaneal lever during running. However, this study had only two breeds of horses because we aimed to collect data from wide range of taxa. To test this idea, it will be necessary to collect data from broad range of species and breeds within Equidae.

There were some possibilities to lead errors in this study. *In vivo* measurement was limited by animal behavior and shooting environment. In addition, the measurements were not performed with any markers directly put on the living specimens. When measuring skeletal specimens, although the articulation flexibility is small, thickness of the adhesive material could cause errors, and the effect of measurement tools accuracy also coursed errors. The ideas to avoid these errors, such as using motion capture, making a strait walkway for recording video, and taking video with x-ray cinematography. Furthermore, no speed-related parameters, such as actual velocity, Froude number, or duty factor, were measured in this study. Although all animals were observed walking at self-selected speeds, variation in walking velocity among species may have affected joint postures. Therefore, the lack of speed standardization represents a limitation when comparing θ_{obs} values across taxa. Future studies may benefit from quantifying stride parameters to better control for interspecific variation in locomotor dynamics.

CONCLUSION

In this study, we proposed a mechanical model of the ankle extensor apparatus of terrestrial mammals that approximates the ankle joint as a simple hinge and the force of the ankle extensors as acting parallel to the tibia. Our model predicts an estimated joint angle (θ_{est}) at which the moment arm of the ankle extensors is maximized. By comparing this predicted angle with observed ankle joint angles (θ_{obs}) during walking, we found that despite large variations in θ_{obs} among species, mechanical advantage of the calcaneal lever (sin a) remains within a relatively narrow range, supporting the notion that, across taxa, skeletal morphology at the ankle joint has been selected for optimization of mechanical advantage of the calcaneal lever for the ankle plantar flexors. This hypothesis is supported even in species with varying ankle joint postures and ranges of motion. This insight provides a new perspective for reconstructing locomotor postures in extinct terrestrial mammals and enhances understanding of the biomechanical constraints shaping limb function.

ACKNOWLEDGEMENTS

Fukuzumi (University of Tsukuba) for providing helpful advice. We also thank reviewers for helping to improve this article.

ADDITIONAL INFORMATION AND DECLARATIONS

Competing Interests
The authors declare that they have no competing interests.

Author Contributions
- Fumihiro Mizuno conceived and designed the experiments, performed the experiments, analyzed the data, prepared figures and/or tables, authored or reviewed drafts of the article, and approved the final draft.
- Shin-ichi Fujiwara conceived and designed the experiments, authored or reviewed drafts of the article, and approved the final draft.

Animal Ethics
The following information was supplied relating to ethical approvals (*i.e.*, approving body and any reference numbers):

This study videotaped mammals from visitor-viewing route and no treatment.

We followed the ethical guidelines of National Museum of Nature and Science (Tokyo) for dissection.

Data Availability
The following information was supplied regarding data availability:

The raw measurements are available in the Supplemental Files.

Supplemental Information
Supplemental information for this article can be found online at http://dx.doi.org/10.7717/peerj.20056#supplemental-information.

REFERENCES

Alexander RM. 1991. Energy-saving mechanisms in walking and running. *Journal of Experimental Biology* **160**:55–69 DOI 10.1242/jeb.160.1.55.

Alexander RM, Jayes AS. 1978a. Optimum walking techniques for idealized animals. *Journal of Zoology* **186(1)**:61–81 DOI 10.1111/j.1469-7998.1978.tb03357.x.

Alexander RM, Jayes AS. 1978b. Vertical movements in walking and running. *Journal of Zoology* **185(1)**:27–40 DOI 10.1111/j.1469-7998.1978.tb03311.x.

Alexander RM, Jayes AS. 1983. A dynamic similarity hypothesis for the gaits of quadrupedal mammals. *Journal of Zoology* **201(1)**:135–152 DOI 10.1111/j.1469-7998.1983.tb04266.x.

Alexander RM, Vernon A. 1975. The mechanics of hopping by kangaroos (Macropodidae). *Journal of Zoology* **177(2)**:265–303 DOI 10.1111/j.1469-7998.1975.tb05983.x.

Biewener AA. 1989. Scaling body support in mammals: limb posture and muscle mechanics. *Science* **245(4913)**:45–48 DOI 10.1126/science.2740914.

Biewener AA. 1990. Biomechanics of mammalian terrestrial locomotion. *Science* **250(4984)**:1097–1103 DOI 10.1126/science.2251499.

Biewener AA. 1998. Muscle-tendon stresses and elastic energy storage during locomotion in the horse. *Comparative Biochemistry and Physiology-B Biochemistry and Molecular Biology* **120(1)**:73–87 DOI 10.1016/S0305-0491(98)00024-8.

Biewener AA, Roberts TJ. 2000. Muscle and tendon contributions to force, work, and elastic energy savings: a comparative perspective. *Exercise and Sport Sciences Reviews* **28(3)**:99–107.

Blickhan R, Full RJ. 1993. Similarity in multilegged locomotion: bouncing like a monopode. *Journal of Comparative Physiology A* **173(5)**:509–517 DOI 10.1007/BF00197760.

Bower MA, McGivney BA, Campana MG, Gu J, Andersson LS, Barrett E, Davis CR, Mikko S, Stock F, Voronkova V, Bradley DG, Fahey AG, Lindgren G, MacHugh DE, Sulimova G, Hill EW. 2012. The genetic origin and history of speed in the thoroughbred racehorse. *Nature Communications* **3(1)**:360 DOI 10.1038/ncomms1644.

Cavagna GA, Heglund NC, Taylor CR. 1977. Mechanical work in terrestrial locomotion: two basic mechanisms for minimizing energy expenditure. *American Journal of Physiology-Regulatory, Integrative and Comparative Physiology* **233(5)**:R243–R261 DOI 10.1152/ajpregu.1977.233.5.R243.

Cunningham P. 1991. The genetics of thoroughbred horses. *Scientific American* **264(5)**:92–98 DOI 10.1038/scientificamerican0591-92.

Day LM, Jayne BC. 2007. Interspecific scaling of the morphology and posture of the limbs during the locomotion of cats (Felidae). *The Journal of Experimental Biology* **210(4)**:642–654 DOI 10.1242/jeb.02703.

Deforth M, Zwicky L, Horn T, Hintermann B. 2019. The effect of foot type on the Achilles tendon moment arm and biomechanics. *Foot* **38(3)**:91–94 DOI 10.1016/j.foot.2018.10.003.

Dimery NJ, Alexander RMN, Ker RF. 1986. Elastic extension of leg tendons in the locomotion of horses (Equus caballus). *Journal of Zoology* **210(3)**:415–425 DOI 10.1111/j.1469-7998.1986.tb03646.x.

Dutto DJ, Hoyt DF, Clayton HM, Cogger EA, Wickler SJ. 2006. Joint work and power for both the forelimb and hindlimb during trotting in the horse. *The Journal of Experimental Biology* **209(20)**:3990–3999 DOI 10.1242/jeb.02471.

Engberg I, Lundberg A. 1969. An electromyographic analysis of muscular activity in the hindlimb of the cat during unrestrained locomotion. *Acta Physiologica Scandinavica* **75(4)**:614–630 DOI 10.1111/j.1748-1716.1969.tb04415.x.

Fischer MS, Schilling N, Schmidt M, Haarhaus D, Witte H. 2002. Basic limb kinematics of small therian mammals. *Journal of Experimental Biology* **205(9)**:1315–1338 DOI 10.1242/jeb.205.9.1315.

Fujiwara S. 2009. Olecranon orientation as an indicator of elbow joint angle in the stance phase, and estimation of forelimb posture in extinct quadruped animals. *Journal of Morphology* **270(9)**:1107–1121 DOI 10.1002/jmor.10748.

Fujiwara S, Hutchinson JR. 2012. Elbow joint adductor moment arm as an indicator of forelimb posture in extinct quadrupedal tetrapods. *Proceedings of the Royal Society B: Biological Sciences* **279(1738)**:2561–2570 DOI 10.1098/rspb.2012.0190.

Garland T, Dickerman AW, Janis CM, Jones JA. 1993. Phylogenetic analysis of covariance by computer simulation. *Systematic Biology* **42(3)**:265–292 DOI 10.1093/sysbio/42.3.265.

Geyer H, Seyfarth A, Blickhan R. 2006. Compliant leg behaviour explains basic dynamics of walking and running. *Proceedings of the Royal Society B: Biological Sciences* **273(1603)**:2861–2867 DOI 10.1098/rspb.2006.3637.

Gnagey L, Clayton HM, Lanovaz JL. 2006. Effect of standing tarsal angle on joint kinematics and kinetics. *Equine Veterinary Journal* **38(7)**:628–633 DOI 10.2746/042516406X159043.

Goslow GE, Reinking RM, Stuart DG. 1973. The cat step cycle: hind limb joint angles and muscle lengths during unrestrained locomotion. *Journal of Morphology* **141(1)**:1–41 DOI 10.1002/jmor.1051410102.

Goslow GE, Seeherman HJ, Taylor CR, McCUTCHlN MN, Heglund NC. 1981. Electrical activity and relative length changes of dog limb muscles as a function of speed and gait. *Journal of Experimental Biology* **94(1)**:15–42 DOI 10.1242/jeb.94.1.15.

Gray J. 1944. Studies in the mechanics of the tetrapod skeleton. *Journal of Experimental Biology* **20(2)**:88–116 DOI 10.1242/jeb.20.2.88.

Gregory WK. 1912. Notes on the principles of quadrupedal locomotion and on the mechanism of the limbs in hoofed animals. *Annals of the New York Academy of Sciences* **22(1)**:267–294 DOI 10.1111/j.1749-6632.1912.tb55164.x.

Griffin TM, Main RP, Farley CT. 2004. Biomechanics of quadrupedal walking: how do four-legged animals achieve inverted pendulum-like movements? *Journal of Experimental Biology* **207(20)**:3545–3558 DOI 10.1242/jeb.01177.

Hildebrand M. 1984. Rotations of the leg segments of three fast-running cursors and an elephant. *Journal of Mammalogy* **65(4)**:718–720 DOI 10.2307/1380866.

Hildebrand M, Hurley JP. 1985. Energy of the oscillating legs of a fast-moving cheetah, pronghorn, jackrabbit, and elephant. *Journal of Morphology* **184(1)**:23–31 DOI 10.1002/jmor.1051840103.

Inuzuka N. 1996. Preliminary study on kinematic gait analysis in mammals. *Mammal Study* **21(1)**:43–57 DOI 10.3106/mammalstudy.21.43.

Jones ME, Travouillon K, Janis CM. 2024. Proportional variation and scaling in the hindlimbs of hopping mammals, including convergent evolution in argygrolagids and jerboas. *Journal of Mammalian Evolution* **31(1)**:1–16 DOI 10.1007/s10914-023-09699-9.

Kato Y, Yamauchi S. 2003. *Comparative anatomy of domestic animals.* Vol. 1. Tokyo: Yokendo.

König HE, Liebich H-G, Bragulla H. 2007. *Veterinary anatomy of domestic mammals: textbook and colour atlas.* Stuttgart, Germany: Schattauer Verlag.

Manter JT. 1938. The dynamics of quadrupedal walking. *Journal of Experimental Biology* **15(4)**:522–540 DOI 10.1242/jeb.15.4.522.

McGowan CP, Baudinette RV, Biewener AA. 2005. Joint work and power associated with acceleration and deceleration in tammar wallabies (Macropus eugenii). *The Journal of Experimental Biology* **208(1)**:41–53 DOI 10.1242/jeb.01305.

McGowan CP, Collins CE. 2018. Why do mammals hop? Understanding the ecology, biomechanics and evolution of bipedal hopping. *Journal of Experimental Biology* **221(12)**:69 DOI 10.1242/jeb.161661.

Mizuno F, Kohno N. 2023. New genicular joint angle criteria for flexor muscle (*Musculus semimembranosus*) during the terrestrial mammals walking. *PeerJ* **11**:e15379 DOI 10.7717/peerj.15379.

Nakagawa T. 2014. The histroy and reservation of Kiso horse. *Livestock Technology* **711**:15–19 DOI 10.57546/livestocktechnology.2014.711-Aug._15 (in Japanese).

Nicolopoulos-Stournaras S, Iles JF. 1984. Hindlimb muscle activity during locomotion in the rat (Rattus norvegicus) (Rodentia: Muridae). *Journal of Zoology* **203(3)**:427–440 DOI 10.1111/j.1469-7998.1984.tb02342.x.

Nozawa K. 1992. Origin and ancestry of native horses in eastern Asia and Japan. *Japanese Journal of Equine Science* **3(1)**:1–18 DOI 10.1294/jes1990.3.1.

O'Connor SM, Dawson TJ, Kram R, Donelan JM. 2014. The kangaroo's tail propels and powers pentapedal locomotion. *Biology Letters* **10(7)**:1–5 DOI 10.1098/rsbl.2014.0381.

Patel BA, Horner AM, Thompson NE, Barrett L, Henzi SP. 2013. Ontogenetic scaling of fore- and hind limb posture in wild chacma baboons (Papio hamadryas ursinus). *PLOS ONE* **8(7)**:1–8 DOI 10.1371/journal.pone.0071020.

Polly PD. 2007. Limbs in mammalian evolution. In: Hall BK, ed. *Fins into Limbs: Ecolution, Development, and Transformation*. Chicago: University of Chicago Press, 245–268.

Rasmussen S, Chan AK, Goslow GE. 1978. The cat step cycle: electromyographic patterns for hindlimb muscles during posture and unrestrained locomotion. *Journal of Morphology* **155(3)**:253–269 DOI 10.1002/jmor.1051550302.

Ray SF, Takahashi KZ. 2020. Gearing up the human ankle-foot system to reduce energy cost of fast walking. *Scientific Reports* **10(1)**:1–12 DOI 10.1038/s41598-020-65626-5.

R Core Team. 2024. *R: a language and environment for statistical computing*. Version 4.4.1. Vienna: R Foundation for Statistical Computing. *Available at https://www.r-project.org*.

Ren L, Butler M, Miller C, Paxton H, Schwerda D, Fischer MS, Hutchinson JR. 2008. The movements of limb segments and joints during locomotion in African and Asian elephants. *Journal of Experimental Biology* **211(17)**:2735–2751 DOI 10.1242/jeb.018820.

Revell LJ. 2012. phytools: an R package for phylogenetic comparative biology (and other things). *Methods in Ecology and Evolution* **3(2)**:217–223 DOI 10.1111/j.2041-210X.2011.00169.x.

Walmsley B, Hodgson JA, Burke RE. 1978. Forces produced by medial gastrocnemius and soleus muscles during locomotion in freely moving cats. *Journal of Neurophysiology* **41(5)**:1203–1216 DOI 10.1152/jn.1978.41.5.1203.

Whelan PJ, Hiebert GW, Pearson KG. 1995. Stimulation of the group I extensor afferents prolongs the stance phase in walking cats. *Experimental Brain Research* **103(1)**:20–30 DOI 10.1007/BF00241961.

Windsor DE, Dagg AI. 1971. The gaits of the Macropodinae (Marsupialia). *Journal of Zoology* **163(2)**:165–175 DOI 10.1111/j.1469-7998.1971.tb04530.x.

Yamashita D. 2014. About the native horses of Japan. *Livestock Technology* **710**:34–39 DOI 10.57546/livestocktechnology.2014.710-Jul._34 (in Japanese).